

See discussions, stats, and author profiles for this publication at: <https://www.researchgate.net/publication/231396758>

Observations of Molecular Rydberg State Decay for $n = 10-200$

ARTICLE *in* THE JOURNAL OF PHYSICAL CHEMISTRY · MARCH 1994

Impact Factor: 2.78 · DOI: 10.1021/j100064a032

CITATIONS

39

READS

16

3 AUTHORS, INCLUDING:



Uzi Even

Tel Aviv University

176 PUBLICATIONS 5,321 CITATIONS

SEE PROFILE



Raphael D. Levine

Hebrew University of Jerusalem

200 PUBLICATIONS 4,899 CITATIONS

SEE PROFILE

Observations of Molecular Rydberg State Decay for $n = 10\text{--}200$

U. Even*

School of Chemistry, Tel Aviv University, Tel Aviv 60978, Israel

R. D. Levine

The Fritz Haber Research Center for Molecular Dynamics, The Hebrew University of Jerusalem, Jerusalem 91904, Israel

R. Bersohn

*Department of Chemistry, Columbia University, New York, New York 10027**Received: October 15, 1993; In Final Form: December 27, 1993**

Time-resolved ZEKE (zero electron kinetic energy) spectroscopy has enabled measurements of the rates of decay of molecular Rydberg states close to (within a few cm^{-1} of) the ionization threshold. The ion yield as a function of photon energy in this region cannot be understood without knowing both the ionization potential and the principal quantum numbers, n , of the states involved. Unfortunately, these two unknowns are linked by the equation $h\nu = \text{IP} - R/(n - \delta)^2$; an independent method must be used to measure the ionization potential, IP. We have found two molecules appropriate for these measurements, bis(benzene)chromium (BBC) and diazacyclooctane (DABCO), both of which have very long Rydberg series with resolved transitions up to $n = 35$ (BBC) and $n = 70$ (DABCO). Highly accurate values of the ionization potential ($\pm 0.5 \text{ cm}^{-1}$) were obtained by extrapolating these series. The line widths are shown to decrease with increasing n with a power of n of 2.5 ± 0.3 . These are the first measurements of the n dependence of the nonradiative rates over a large range of n for polyatomic molecules in Rydberg states. However, one cannot simply extrapolate the lifetimes (as determined from the widths) to the region near the ionization threshold where the $n = 100\text{--}200$ states are being excited. There the lifetimes as determined directly by ZEKE spectroscopy are longer by several orders of magnitude than the values obtained by extrapolation.

Introduction

Our longtime friend and colleague, Joshua Jortner, has an abiding interest in the nonradiative decay of electronically excited states. The time evolution of high-lying Rydberg states is a particularly important example of a nonradiative process. The primary process is a decay to lower energy electronic states with concomitant increase of nuclear energy of the core. It is well-known that, just below the ionization continuum a second channel, autoionization, opens in which the electron acquires sufficient energy from the nuclear modes to escape.^{1–6} From the very start of our work on the very high n states, Joshua emphasized to us the need for an independent determination of the ionization potential in order to assess reliably the importance of this second channel. He has also been very interested in the question of the change in the decay mechanism as one spans the entire range of n values. We hope that the work reported herein provide a first step toward these two goals.

Rydberg states are commonly defined as states whose principal quantum numbers exceed those of the valence electrons. As this principal quantum number, n , increases their wave functions become ever more extended; the electron is typically found at a large distance from the positively charged, polarizable core. The absorption bands due to transitions to Rydberg states fit the equation

$$h\nu = \text{IP} - R/(n - \delta)^2 \quad (1)$$

where IP is the ionization potential, R is the Rydberg constant $109\,737.3 \text{ cm}^{-1}$, and δ is the quantum defect. Series of Rydberg transitions have been found for every atom but are clearly resolved only in a minority of polyatomic molecules. Even for these, only

the first few members of the series are, in general, observable. The basic problem is that, even when the lower members are relatively sharp, the higher Rydberg transitions are obscured by numerous overlapping Rydberg series and by intervalence transitions which are dissociative and therefore extremely broad.

A truly isolated atom in a Rydberg state below the first ionization limit can change state only by radiative processes. However, an isolated molecule in a Rydberg state can change state by radiationless processes as well. A general framework for describing the exchange of energy and angular momentum between a Rydberg electron and a molecular ion core has been developed by Fano¹ and others.² It has been applied in greatest detail to experimental studies of H_2 , and the observed energies, intensities, and shapes of the lines of Rydberg series are in excellent agreement with calculations.^{1–4} However, applications to polyatomic molecules have been few and generally semiquantitative in nature due to their much greater complexity.⁵ The central aim of the research reported here was to study the dynamics of polyatomic molecular Rydberg states, that is, the rate at which they decay by radiationless processes and the mechanisms of these processes. A number of experiments have shown that the line widths of Rydberg transitions to states n decrease rapidly with increasing n . For example, Grubb et al. found that the widths of a Rydberg series in benzene decrease from 82 cm^{-1} for the transition to the $n = 3$ state to 6 cm^{-1} for the transition to the $n = 7$ state.⁸ Reiser et al. found high-lying, long-lived Rydberg states in NO .² Inasmuch as the line shapes are Lorentzian, it is inferred that the line widths are lifetime limited. It is generally accepted that the reason for the decrease in rate constant with increasing n is that the further the electron is, on average, from the molecular ion, the less strongly it interacts.

To study the dependence on n of the dynamics, one needs a molecule for which a really extended Rydberg series can be

* Abstract published in *Advance ACS Abstracts*, March 1, 1994.

observed. So far, two such molecules have been found, BBC (bis(benzene)chromium) and DABCO (1,4-diazabicyclo[2.2.2]octane). Previous workers had found, using nonlaser light sources, that BBC exhibits a Rydberg series from $n = 4$ to 12.^{9,10} Aside from some degree of chemical instability, this molecule is ideal for these studies. The highest occupied molecular orbital of BBC is occupied by two electrons localized in the chromium $3d_z^2$ nonbonding state. In general, transitions originating from a nonbonding state are not accompanied by changes in vibrational quantum numbers. The ionization potential of BBC, 5.45 eV, is so low that many lower n members of the Rydberg series can be observed before they are obscured by transitions of the bonding electrons. An additional convenience is that, after excitation of the Rydberg state and subsequent radiationless transition, the molecule dissociates into two benzene molecules and a Cr atom. The latter is then detected with great sensitivity by two photon ionization.

Three Rydberg series have been found in DABCO with n values as high as 41.^{11,12} These were detected by two-photon resonant ionization. The molecules were excited to a resonant S_1 transition with an excess vibrational energy of 1007 cm^{-1} above the S_1 origin; the wavelength of a second photon was then scanned across the autoionizing Rydberg lines, producing ions and low-energy electrons that can be easily detected.

The use of an expansion cooled beam is critical to the success of the experiments. This is particularly true for large molecules such as BBC and DABCO which have respectively 69 and 54 vibrational modes. Extreme cooling is needed so that higher members of the Rydberg series are not smeared out by hot bands originating from thermally vibrationally excited molecules.

Experimental Section

The molecules were cooled in a supersonic expansion from a heated pulsed valve.¹³ A three-chamber, differentially pumped system was used which contained both ion time of flight mass and ZEKE spectrometers. The molecular beam was skimmed twice. A backing pressure of 2 atm of He with a conical nozzle of 0.5 mm diameter generated sufficient cooling even for large molecules.¹⁴ We estimate the rotational temperature to be 1–4 K. The easily decomposing BBC molecule was heated to 125°C and DABCO to 100°C in the valve. The BBC molecules were excited simultaneously by two tunable dye lasers (Lambda Physik FL 2002) pumped by a single excimer laser (Lambda Physik 150 MSC). One laser frequency was doubled in a BBO (barium metaborate) crystal to cover the range of 226–235 nm. The excited molecule decomposes to release chromium atoms that were detected by R2PI (resonant two-photon ionization) of the second laser, tuned to the $\{a^7S_3 \rightarrow y^7P_0\}$ chromium transition at 357.869 nm. Care was taken to prevent multiphoton processes other than those desired. The absorption spectrum of the molecule was monitored by following the intensity of the chromium ion in the mass spectrometer. Using this method, we could monitor the molecular absorption of a series of lines that could be fitted to the Rydberg formula, eq 1, from $n = 10$ to $n = 35$. The width of these lines could be measured by fitting to a Lorentzian shape up to $n = 20$ at which point the line width was mainly determined by the laser width (0.4 cm^{-1}) and the rotational width. Higher Rydberg states were monitored using a ZEKE spectrometer. This spectrometer consisted of two parallel, gold-plated, 100 mm diameter plates separated by 10 mm. A fast ($\sim 10\text{ ns}$), 30-V pulse was applied after a controllable delay to one of these plates, field ionizing the large n Rydbergs, and the resulting electrons were detected by a multichannel plate detector placed near the exit mesh in the other, grounded plate. The short flight time of the electrons allowed us to separate the prompt electrons (resulting from photoexcitation of the metal parts and residual molecules in the vacuum) from those created by the delayed field. A weak constant field (0.1 V/cm) swept out the prompt electrons. The

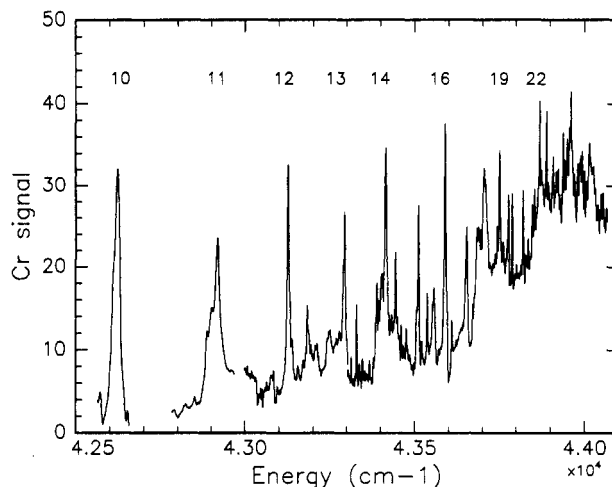


Figure 1. R2PI excitation spectrum of BBC in the wavelength region 227–235 nm. Some transitions are labeled by the Rydberg state quantum number n . Note the decrease in widths from $n = 10, 11$ to $n = 19, 22$.

shortest practical delay was 100 ns. We monitored the intensity of the electron signal as a function of the delayed (100–5000 ns) extraction pulse and interpreted it to indicate the decay of the population in the laser excited high Rydberg state. A nonexponential decay was observed and was fitted to a sum of two decaying exponentials.¹⁵ The faster component was taken to be an indicator of the intramolecular relaxation of these high Rydbergs and was compared with the lifetime extracted from the line width of the lower Rydberg states.

The DABCO molecules were studied by a similar procedure. One laser was tuned to a vibrationally excited state in the S_1 manifold (1007 cm^{-1} above the origin at 271.73 nm) in the Q rotational branch (which is the most intense line in the rotational contour). The other laser was scanned from the $n = 10$ Rydberg line to the IP producing both ions and slow electrons. In all cases the extraction field was applied after the laser excitation so that the molecular excitation occurred in a field-free volume (except for the 0.1 V/cm prompt electron sweep field).

Results

Figure 1 is an overall view of the BBC spectrum from 227 to 235 nm which covers Rydberg transitions from $n = 10$ to 22. It is a chromium atom two-photon ionization excitation spectrum and not an absorption spectrum. However, the excitation spectrum of the laser-induced fluorescence of the Cr atoms in this wavelength range was previously shown to be identical in shape to the absorption spectrum.¹⁰ In all, transitions from $n = 4$ to 35 were identified. Table 1 contains a list of observed frequencies (corrected from air to vacuum) and frequencies calculated from eq 1, an assumed n , a value of $44\,103.3\text{ cm}^{-1}$ for the IP and 1.375 for the quantum defect. The agreement is remarkable, and it is estimated that the probable error in the ionization potential is only 0.5 cm^{-1} .

Having established the position of the Rydberg transitions, the next step was to measure the widths. This could not be done for every n because some lines fall close enough to other transitions that it was difficult to define their widths. In other cases the signal/noise was too poor. Figure 2 is a plot of some representative Rydberg bands of DABCO superimposed to show the progressive narrowing with increasing n . Figure 3 is a log–log (base 10) plot of the widths in BBC against n . The widths defined as the full widths at half-maximum have been corrected for the 0.4 cm^{-1} width of the laser and the 0.5 cm^{-1} rotational width by taking the true width to be the square root of the square of the observed width minus the squares of the laser and rotational widths. The observed widths decreased from 37 cm^{-1} for the $n = 5$ transition to 0.8 cm^{-1} for the $n = 20$ transition. The straight line in Figure

TABLE 1: Calculated and Observed Energy Levels of Rydberg States of DABCO and BBC

<i>n</i>	energies (cm ⁻¹)					
	DABCO			BBC		
	obsd	calcd	diff	obsd	calcd	diff
11	58094.2	58094.6	-0.4			
12	58255.4	58256.0	-0.6	43113.4	43117.3	-3.9
13	58379.1	58380.5	-1.4	43280.8	43277.6	3.2
14	58477.4	58478.6	-1.2	43402.5	43401.3	1.2
15	58556.9	58557.2	-0.3	43498.6	43498.7	-0.1
16	58620.9	58621.2	-0.3	43575.8	43576.9	-1.1
17	58673.5	58673.9	-0.4	43638.4	43640.5	-2.1
18	58717.5	58718.0	-0.5	43691.4	43693.0	-1.6
19	58754.5	58755.1	-0.6	43737.1	43736.8	0.3
20	58786.5	58786.6	-0.1	43774.8	43773.8	1.0
21	58822.2	58813.7	8.5	43806.6	43805.2	1.4
22	58843.4	58837.1	6.3	43833.7	43832.2	1.5
23	58856.1	58857.5	-1.4	43855.2	43855.5	-0.3
24	58874.6	58875.4	-0.8	43875.1	43875.8	-0.7
25	58890.5	58891.1	-0.6	43894.5	43893.6	0.9
26	58904.5	58905.0	-0.5	43909.3	43909.3	0.0
27	58917.1	58917.3	-0.2	43924.0	43923.1	0.9
28	58928.4	58928.4	0.0	43935.6	43935.4	0.2
29	58936.5	58938.3	-1.8	43946.4	43946.5	-0.1
30	58945.7	58947.2	-1.5	43956.4	43956.3	0.1
31	58953.9	58955.3	-1.4	43965.9	43965.2	0.7
32	58961.2	58962.6	-1.4	43973.4	43973.3	0.1
33	58967.9	58969.2	-1.3	43979.9	43980.5	-0.6
34	58974.1	58975.3	-1.2	43986.0	43987.2	-1.2
35	58979.8	58980.8	-1.0	43992.6	43993.2	-0.6
36	58985.1	58985.9	-0.8			
37	58990.0	58990.5	-0.5			
38	58994.2	58994.9	-0.7			
39	58998.3	58998.8	-0.5			
40	59002.1	59002.5	-0.4			
41	59005.8	59005.9	-0.1			
42	59009.0	59009.1	-0.1			
43	59012.0	59012.0	0.0			
44	59014.7	59014.8	-0.1			
45	59017.3	59017.3	0.0			
46	59019.8	59019.7	0.1			
47	59022.0	59022.0	0.0			
48	59024.2	59024.1	0.1			
49	59026.2	59026.0	0.2			
50	59028.0	59027.9	0.1			
51	59029.8	59029.6	0.2			
52	59031.5	59031.3	0.2			
53	59033.0	59032.8	0.2			

IP 59072.5 ± 0.3 cm⁻¹ (DABCO), 44090.3 ± 0.5 cm⁻¹ (BBC)

δ 0.407 ± 0.010 (DABCO), 1.38 ± 0.01 (BBC)

3 has a slope of 2.5 ± 0.3 . These widths are assumed to be lifetime limited, that is, determined from the uncertainty principle.

In BBC Rydberg transitions to states with $n > 35$ were obscured by intervalence transitions. In other words, the excited valence states also dissociate into Cr atoms and absorptions to these states are stronger than those to the Rydberg states. Close to the IP, perhaps 10 cm⁻¹ below it where n is about 100, another phenomenon can be exploited to measure the lifetime of the unresolved Rydberg state. If a molecule is excited to a state just below its ionization potential, only a relatively small external electric field is required to extract an electron and produce a positive ion. In the ZEKE technique the molecule is photoexcited below its ionization potential.¹⁶ Any electrons that are produced promptly are either derived from the walls of the apparatus or from molecules which can autoionize because their core has some internal energy. A very crude estimate of their density is 1000/cm³. These prompt electrons reach the detector first. After a certain delay time, a pulsed electric field is applied which extracts the "zero energy" electrons. The variation of this signal with the delay between the light pulse and the electric field pulse yields the lifetime of the particular Rydberg state. After a long enough

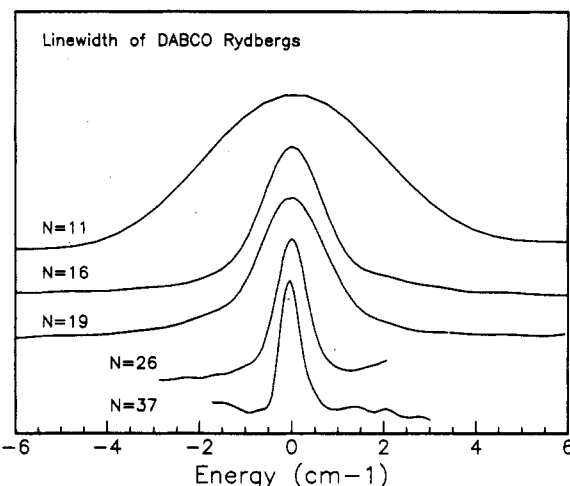


Figure 2. A representative sample of line shapes in DABCO shown on an enlarged scale to exhibit their generally Lorentzian line shape and decrease in widths with increasing n .

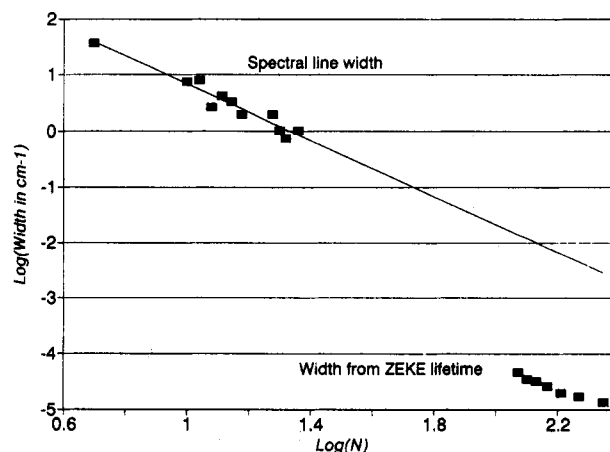


Figure 3. A log-log plot (base 10) of the widths of the transitions to Rydberg states N of BBC versus N . The slope of the least-squares fitted straight line is 2.5 ± 0.3 .

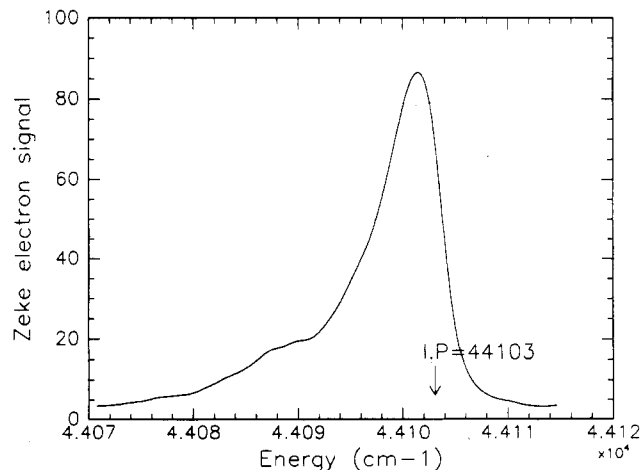


Figure 4. ZEKE spectrum of BBC taken with a delay of 200 ns between the optical and electric field pulses. The field was 30 V/cm. The intensity has begun to decrease slightly below the IP, perhaps because of rotational autoionization.

time the molecule will no longer be in this easily ionizable Rydberg state; instead some of the electronic energy will have been converted into vibrational energy of the core.

The ZEKE signal of BBC shown in Figure 4 was obtained at a 200-ns delay using an extracting field of 30 V/cm and preexcitation field of 0.1 V/cm. The signal disappears shortly

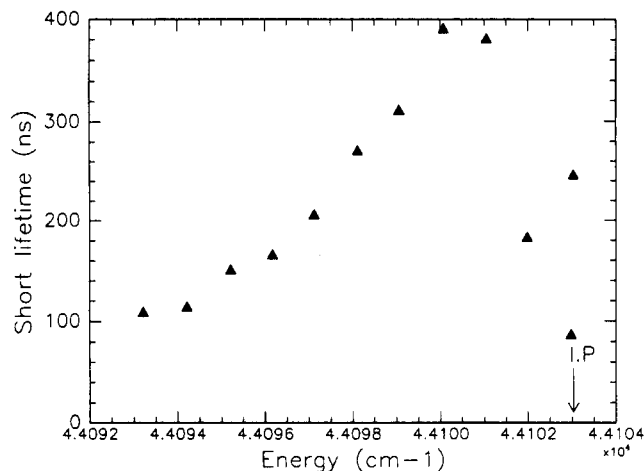


Figure 5. Lifetime of the Rydberg states of BBC close to its IP. The lifetimes continue to lengthen with increasing n but slower than at lower n until just below the IP. Beyond the IP the signal sharply decreases and the lifetimes become too short to measure with a ns laser.

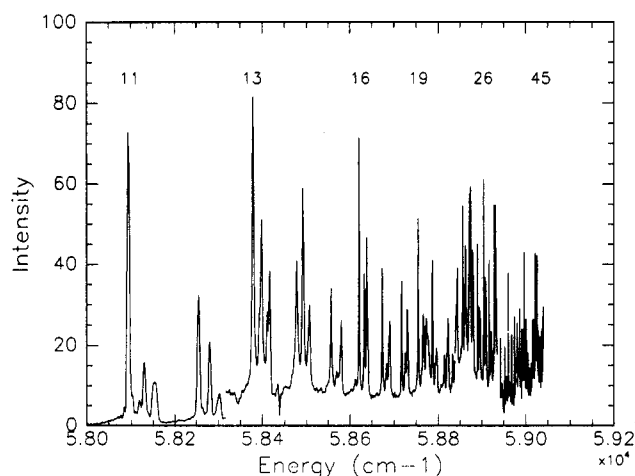


Figure 6. Rydberg series for DABCO for $n = 11$ to $n = 45$ using resonant two-photon simultaneous two-color ionization. The spectrum was obtained by exciting the molecule to an intermediate state of the S_1 vibronic manifold (1007 cm^{-1} excess energy) and scanning the ionizing laser. Slow electrons were collected after a delay of 200 ns.

above the IP because the autoionization rate increases with increasing energy. IP is defined in this paper as the asymptotic value derived by extrapolating the frequencies of eq 1 to infinite n . Bahatt et al. found that, in the aromatic molecules phenanthrene, perylene, 9,10-dichloroanthracene, and aniline, the ZEKE measured lifetime steadily increases with increasing energy but very near the IP suddenly begins to decrease.¹⁷ The same behavior is exhibited by BBC as shown in Figure 5. Chupka has argued that the decrease is due to the extreme sensitivity of the very high lying Rydberg states to external fields and collisions which are present to some degree in every system.¹⁸ In other words, contrary to what is stated here, the decrease of intensity after the ZEKE peak would be due primarily to external rather than internal causes. However, in the same apparatus, under the same pressures and stray fields the time behavior of atomic Hg is quite different.¹⁹ Its time dependence is seen only on the microsecond time scale, an order of magnitude longer than for the molecules discussed here. On that longer time scale the atomic Rydberg lifetime is governed by collisions and finite residence time of the beam in our apparatus.

Results for DABCO are shown in Figures 6–8. Figure 6 presents the Rydberg spectrum of DABCO from $n = 11$ to $n = 45$ and Figure 7 from $n = 45$ to $n = 70$ where the level spacing approaches the laser width. Note the change in the vertical scale as the ZEKE peak is approached, an indication of the longer

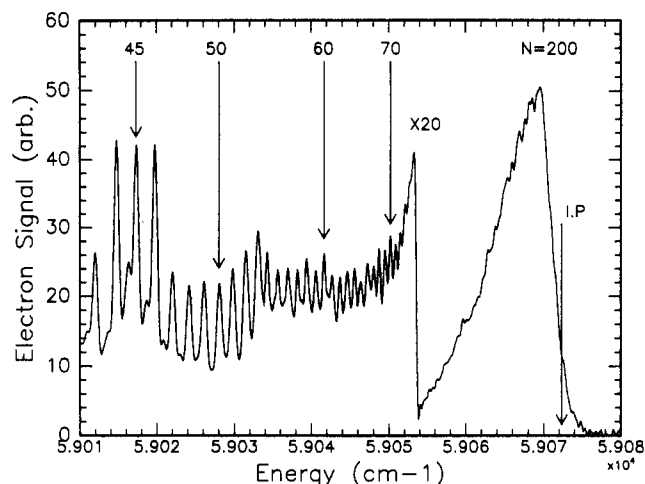


Figure 7. High Rydberg series ($n = 45$ –200) of DABCO, its ZEKE peak, and derived ionization potential. Note the change of scale near $n = 80$. Conditions as in Figure 6.

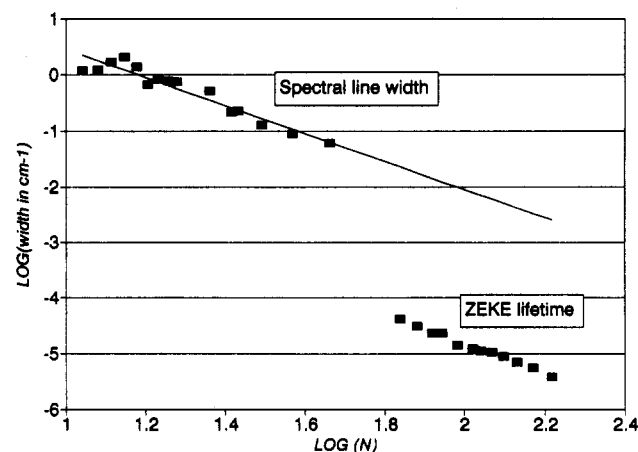


Figure 8. A log-log (base 10) plot of the lifetime of the Rydberg states of DABCO versus n .

lifetime of the ZEKE states. The very long Rydberg series allowed an accurate determination of the vertical ionization potential from the 1007-cm^{-1} vibrational state. Table 1 lists the experimental vacuum corrected wavenumbers and those calculated from eq 1. The IP is $59\,072.5 \pm 0.3\text{ cm}^{-1}$ (vacuum corrected) and the quantum defect is 0.407 ± 0.010 . These data and the electric field allow the determination of the quantum number of the ZEKE peak, $n = 200 \pm 15$. The measured widths and widths inferred from the ZEKE lifetimes are presented in Figure 8. The straight line for the lower n has a slope of 2.5 ± 0.2 .

Discussion

The following considerations appear to be relevant toward an understanding of the n -dependence of the nonradiative rate. First and foremost is the normalization of the wave function of an electron in a Rydberg state with a principal quantum number n . As has been pointed out before,^{2–5,20,21} the normalization is proportional to $n^{-3/2}$ (or, more precisely, to $(n - \delta)^{-3/2}$, where δ is the quantum defect). It follows that a matrix element $\langle n|V|n' \rangle$ connecting two Rydberg states will scale as $(nn')^{-3/2}$ provided that the operator V has a short range so that its dependence on the coordinate of the Rydberg electron does not introduce an additional n -dependence. The potential seen by the Rydberg electron is not purely Coulombic so that n is not an exact quantum number. In the simplest approach one can estimate the rate of nonradiative transitions using the Golden Rule. The electronic part of the rate for a particular $n \rightarrow n'$ transition will be proportional to $|\langle n|V|n' \rangle|^2$ and so will scale as $n^{-3}(n')^{-3}$. If many

final states n' are allowed and/or if the value of n' is only weakly correlated with the value of n , one can sum over all values of n' . Using $E(n) = -R/n^2$ one can write the sum as

$$|\langle n|V|n'\rangle|^2 \simeq \int dE(n') (dn'/dE(n')) |\langle n|V|n'\rangle|^2 \propto n^{-3} \quad (2)$$

The result that, when the range of final states is not very restricted, the transition rate should scale as n^{-3} is consistent with the present results for the widths at the intermediate values of n . The actual power dependence of the nonradiative rates as inferred from the slope of the straight lines in Figures 3 and 8 was 2.5 ± 0.3 and 2.5 ± 0.2 for BBC and DABCO, respectively.

One can understand an n^{-3} scaling law also on classical grounds. The Rydberg electron which moves in an extended Bohr-Sommerfeld elliptical orbit¹⁸ will only be subject to perturbations once per revolution when it passes near the ionic core. Our classical simulations of the motion of a high n electron around a rovibrating core very much verify this intuitive picture.^{22,23} When the use of the Golden Rule is warranted, n must be a nearly good quantum number so that the Rydberg electron can complete at least several revolutions around the core. The rate of transition is then the frequency of the electron passing near the core times the probability that during its pass a change in n will occur.^{17,18} If the latter is only weakly n -dependent, one expects the rate to scale as n^{-3} .

The experimental observation of dissociation products for both BBC and DABCO suggests that eventually the electronic excitation is internally converted to vibrations of the core. If it is the case that, as in the low Rydberg states, there is direct electronic to vibrational energy transfer, the final states n' can be much lower than n . The other physical situation in which the rate will scale as n^{-3} is that of autoionization where the index n' refers to a state of the electron in the continuum.

An important new point shown by these experiments is that the lifetimes as directly measured for the high n states cannot be obtained by a direct extrapolation of the lifetimes as inferred from the measured widths at the intermediate n values. Rather, the lifetimes at the high n values are far longer than an extrapolation of the n^{-3} scaling would suggest (see Figures 3 and 8). The measured line width is but an upper bound to the actual rate of depletion of population from the state n . Hence much of the observed width might be due to dephasing and to transitions which change the magnetic and rotational quantum numbers of the electron, m_l and l , without changing n .^{24,18} This is consistent with our picture of an electron in an elliptical orbit being perturbed only while it passes near the rovibrating core. The optically excited Rydberg state has low l . However, the high n states can couple to the rotating multipolar field of the molecule producing l mixing and thus lengthening the lifetimes considerably. A higher l state corresponds to an orbit staying at longer distances from the molecular core. (Recall the factor r^l in an atomic radial wave function.)

The lifetimes measured by ZEKE spectroscopy are the lifetimes for the disappearance of the initially excited state from the detection window. Note that for a field F of 30 V/cm⁻¹ one expects to ionize all Rydberg states down to about $3.7F^{1/2} \simeq 20$ cm⁻¹ below the ionization potential.²⁵ Hence only when $n' \leq 74$ will the final state n' be out of the field of view. The rate one needs to compute is not $n \rightarrow$ all n' but $n \rightarrow n' < 74$ or n' in the continuum. We shall present such computations elsewhere. Here we merely note that the dependence on n of the lifetimes of the high n states cannot be divorced from the specific details of the experiment.

Bahatt et al. discussed a model in which the lifetime of the ZEKE states scaled as n^6 on the red side of the ZEKE peak (where the lifetime increases with n) and as n^3 times a Boltzmann factor on the blue side of the peak (where the lifetime decreases with n).¹¹ The Boltzmann factor describes the distribution of

rotational energy in the cold molecule. The lifetimes measured in the present experiments scale as n^3 also on the red side of the peak. We do consider that the physics discussed by Bahatt et al. is correct and quite consistent with the present results. As already discussed, the decay rate is determined by the frequency ($\propto n^{-3}$) of revolution around the ionic core times the probability of the transition out of the state n in the core region. The latter scales as n^{-3} for a specific final state n' . It therefore matters very much what final states n' are experimentally distinguishable (by virtue of their failure to ionize when the delayed field is applied). It also matters very much if the high n Rydberg states seen by ZEKE are or are not coupled directly to the vibrations. If the latter, $n' \ll n$ and the overall scaling will be n^{-3} .

In the attempts to derive a scaling law one should note that the use of eq 1 to define n in terms of the known laser frequency and the ionization potential determined from a fit to the intermediate n values, as was done here, is not quite as simple as it looks. The high n Rydberg electron is not moving in a Coulombic potential. At lower n values this can be accounted for by the introduction of an n -independent quantum defect. This is not quite as obvious at the high n values where the electron-core non-Coulombic coupling is of comparable magnitude to the binding energy of the electron. It is these terms that induce the exchange of angular momentum between the electron and the core and thereby bind an electron to a rotationally excited core with the total energy being above the ionization potential.²⁶ The presence of such states is evident in the ZEKE spectrum which extends by a rotational width or so above the IP (see Figures 4 and 7). More work is clearly called for on the definition of the level scheme in the limit just below and just above the ionization threshold.

Conclusion

The major new results of this study are the following:

1. Long Rydberg series were identified in jet-cooled BBC and DABCO molecules enabling an accurate determination of the ionization potential (to ± 0.5 cm⁻¹).
2. The lower n states ($n < 25$) exhibit short decay times, a decay that slows down as n increases with a power law dependence on n .
3. The lifetime varies as n^a where $a = 2.5 \pm 0.3$, close to but different from the expected exponent, $a = 3$.
4. The peaks in the ZEKE spectra are found near $n = 200$.
5. The lifetimes of the high n states ($n > 100$) accessible to ZEKE field ionization spectroscopy are much longer than the values extrapolated from the lifetimes of the lower n 's, by about 2–3 orders of magnitude. Differing probing methods are used in the determination of the lifetimes of low and high n states. The lower n state lifetimes were determined by an energy-resolved method (line broadening) while those of the high n states were determined by a time resolved method. l mixing, induced by external or internal fields, will result in an increased population of many molecular eigenstates of the same n parentage; however, only the small l subset of those are strongly coupled to the core. Dilution lengthening of the nonradiative lifetimes is then expected.²⁷

Acknowledgment. We thank Professor J. Jortner for warm encouragement and numerous helpful discussions. The work was supported by the German-Israel James Franck Program for Laser Matter Interaction (U.E. and R.D.L.) and the US National Science Foundation (R.B.) and Petroleum Research Fund (R.B.).

References and Notes

- (1) Chupka, W. A.; Miller, P. J.; Eyley, E. E. *J. Chem. Phys.* **1988**, *88*, 3032.
- (2) Herzberg, G.; Jungen, Ch. *J. Mol. Spectrosc.* **1972**, *41*, 425.
- (3) Fano, U. *J. Opt. Soc. Am.* **1975**, *65*, 979.
- (4) Dehmer, P. M.; Chupka, W. A. *J. Chem. Phys.* **1976**, *65*, 2243.

- (5) Dill, D.; Jungen, Ch. *J. Phys. Chem.* **1980**, *84*, 2116.
- (6) Resonances in Molecular Photoionization. In *Handbook on Synchrotron Radiation*; Marr, G. V., Ed.; North-Holland: Amsterdam, 1986; Vol. II.
- (7) Grubb, S. G.; Otis, C. E.; Whetten, R. L.; Grant, E. R.; Albrecht, A. C. *J. Chem. Phys.* **1985**, *82*, 1115.
- (8) Reiser, G.; Habenicht, W.; Muller-Dethlefs, K.; Schlag, E. W. *Chem. Phys. Lett.* **1988**, *152*, 119.
- (9) Yu, S.; Ketkov, Domrachev, G. M.; Razuvaev, G. A. *Opt. Spectrosc. (USSR)* **1987**, *63*, 167.
- (10) Penner, A.; Amirav, A.; Tasaki, S.; Bersohn, R. *J. Chem. Phys.* **1993**, *99*, 176.
- (11) Fisanick, G. J.; Eichelberger, T. S.; Robin, M. B.; Kuebler, N. S. *J. Phys. Chem.* **1983**, *87*, 2240.
- (12) Fujii, M.; Ebata, T.; Mikami, N.; Ito, M. *Chem. Phys. Lett.* **1983**, *101*, 578.
- (13) Bahatt, D.; Chesnofsky, O.; Even, U.; Lavie, N.; Magan, Y. *J. Chem. Phys.* **1987**, *91*, 2460.
- (14) Ben-Horin, N.; Even, U.; Jortner, J.; Leutwyler, S. *J. Chem. Phys.* **1992**, *97*, 5296.
- (15) Even, U.; Ben Nun, M.; Levine, R. D. *Chem. Phys. Lett.* **1993**, *210*, 416.
- (16) Muller-Dethlefs, K.; Schlag, E. *Annu. Rev. Phys. Chem.* **1991**, *42*, 109.
- (17) Bahatt, D.; Even, U.; Levine, R. D. *J. Chem. Phys.* **1993**, *98*, 1744.
- (18) Chupka, W. A. *J. Chem. Phys.* **1993**, *98*, 4520; **1993**, *99*, 5800.
- (19) Bahatt, D.; Chesnofsky, O.; Even, U. *Z. Phys. Chem.* **1993**, *40*, 1.
- (20) Bethe, H. A.; Salpeter, E. E. *Handbuch der Physik*; Band XXXV; Springer-Verlag: Berlin, 1957; p 104.
- (21) Bardsley, J. N. *Chem. Phys. Lett.* **1967**, *1*, 229.
- (22) The semiminor and semimajor axes of the ellipse are nka_0 and n^2a_0 , respectively, where a_0 is the Bohr radius and $k = l + 1$ is the parabolic quantum number.
- (23) Rabani, E.; Even, U.; Levine, R. D., to be published.
- (24) Similar considerations apply in other problems where the coupling is not via a low-order resonance, e.g., in the dissociation of van der Waals molecules. See: Jortner, J.; Levine, R. D. *Adv. Chem. Phys.* **1981**, *47*, 1.
- (25) Ya Baranov, L.; Kris, R.; Levine, R. D.; Even, U. *J. Chem. Phys.*, in press.
- (26) Levine, R. D. *Acc. Chem. Res.* **1970**, *3*, 272.
- (27) Jortner, J., private communication.